Development of Clad Boiler Tubes Extruded from Bimetallic Centrifugal Castings*

D.L. Sponseller, G.A. Timmons, and W.T. Bakker

(Submitted 16 April 1996; in revised form 29 October 1997)

Wrought tubes of T-11 steel, externally clad with SS310, have been produced by a new method (U.S. Patent 5,558,150). The alloys were united directly from the molten state by centrifugal casting. In the optimum process, temperatures were controlled to prevent meltback of the SS310 outer layer by the higher melting T-11 stream. Hollow extrusion billets were prepared from the heavy-walled cast bimetallic tubes and successfully hot extruded (at a ratio of 13.4) to 84-mm (3.3 in.) OD × 64-mm (2.5-in.) ID tubes, and (at a ratio of 37.6) to 51-mm (2-in.) OD × 38-mm (1.5-in.) ID tubes. In all, 10 castings were produced, and 12 billets were extruded to tubes. For the most part, thicknesses of the cladding and of the tube wall are rather uniform around the circumference and from end to end of the tubes. Hardness and tensile properties of annealed 51-mm (2-in.) tubes are uniform from end to end of a tube, and between tubes, and readily conform to ASTM A 213; tubes satisfy the flattening and flaring requirements of ASTM A 450. The cladding is metallurgically bonded to the base metal, as revealed by metallography, and by two tests developed for this study: a bond shear strength test and a twist test. In the latter test, rings 3.1 mm (0.125 in.) in thickness are slotted and severely twisted with a special tool. In tubes made by the optimum process, minute fissures that form adjacent to some of the pressure points during twist testing occupy just 3% of the bond-line length. Cost estimates for commercial production of 51-mm (2-in.) tubes via the centrifugal casting route suggest that such tubes should be considerably less expensive than conventionally clad tubes (extruded from composite billets assembled from heavy-walled wrought tubes).

Keywords 1.25Cr-0.5Mo steel, 310 stainless steel, bimetallic tube, boiler tube, centrifugal casting, clad tube, deep sour-gas wells, extrusion, hot corrosion, oxidation, scaling, sulfidation, sulfide stress cracking, superheater tube, ultra super-critical boilers, waste incineration boilers

1. Introduction

Boiler tubes embodying an external stainless steel cladding layer on a carbon or low-alloy steel base offer superior resistance to oxidation or hot corrosion relative to unclad tubes, and provide ensurance against stress-corrosion cracking failure relative to monobloc austenitic stainless tubes. Clad tubes have been used extensively in British utility boilers for well over 20 years (Ref 1, 2). Sidewall tubes with SS310 cladding on carbon steel, for example, have given three-to-ten times the life of unclad tubes in British boilers fired with corrosive high-chlorine coals; as of 1987, 300,000 m (1 million feet) of clad tubes had already been installed. These tubes were produced by extruding composite billets assembled from heavy-walled tubes of the two metals that had been separately processed to billets, pierced, hot reduced, and closely machined prior to assembly into the extrusion billets.

This article describes a new method for preparing extrusion billets, by uniting the two metals directly in the casting stage, via the centrifugal casting process. Extrusion of billets from such castings yields tubes possessing a strong metallurgical bond between the SS310 (25Cr-20Ni) cladding and the T-11 (1.25Cr-0.5Mo) base metal. This direct method of producing the composite billet is expected to lower the cost of clad tubes by a least one third. Such lower cost tubes should be attractive for the following applications in utility boilers:

- High-corrosion areas of existing coal-fired boilers, in both steam-generating tubes and superheaters
- Water walls, screen tubes, and superheater tubes of municipal waste-incineration boilers
- Future boilers designed to achieve higher efficiency levels (i.e., ultra super-critical boilers operating at higher temperatures and pressures)
- Steam-generating tubes of Syngas coolers of integrated coal gasification, electric power-generating plants

2. Centrifugal Casting

To avoid problems of scale-up during eventual commercialization, castings were made with full-scale equipment in a commercial foundry. Ten bimetallic castings were produced: five in each of two separate campaigns. The process entailed simultaneously air melting the SS310 and T-11 alloys, pouring the stainless steel through a tundish into a coated, heavy-walled steel tube spinning rapidly about a horizontal axis, waiting until the stainless steel outer layer had solidified and cooled to a prescribed temperature below its solidus temperature, and then pouring the low-alloy steel through a tundish at the opposite end of the mold. Certain casting parameters were varied from one casting to the next to help optimize the process. The

D.L. Sponseller, ERIM Transportation & Energy Materials Laboratory, Ann Arbor, Michigan; **G.A. Timmons,** Ann Arbor, Michigan; and **W.T. Bakker,** EPRI, Palo Alto, California.

*This paper was originally presented at the ASM International Conference entitled, "Heat-Resistant Materials II," held in Gatlinburg, Tennessee, 11-14 September 1995.

bimetallic castings were 215 mm (8-3/8 in.) in OD, approximately 95 mm (3-3/4 in.) in ID with an outer layer 16 mm (5/8-in.) thick, 2.8 m (111 in.) in length, and weighed about 625 kg (1375 lb) each. A typical casting is shown in Fig. 1. Four castings were made with flux between the layers. This practice, however, is considered neither necessary nor desirable. In the optimum process, the SS310 outer layer is cooled well below its solidus temperature before introduction of the T-11 inner layer. This is done to avoid partial remelting of the stainless steel outer layer by the impinging stream of the considerably higher melting low-alloy steel. Chemical compositions of the four castings described in this article are presented in Table 1.

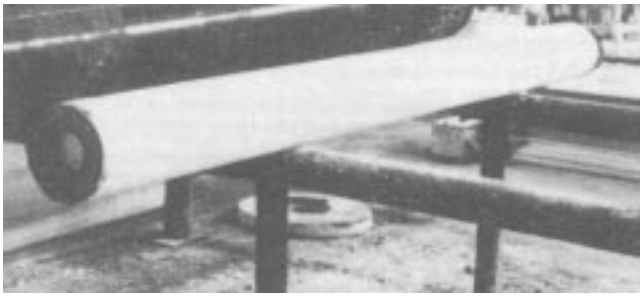

Fig. 1 Casting 10, 2.8 m (9.3 ft) long, about 20 min after removal from mold. 0.05×

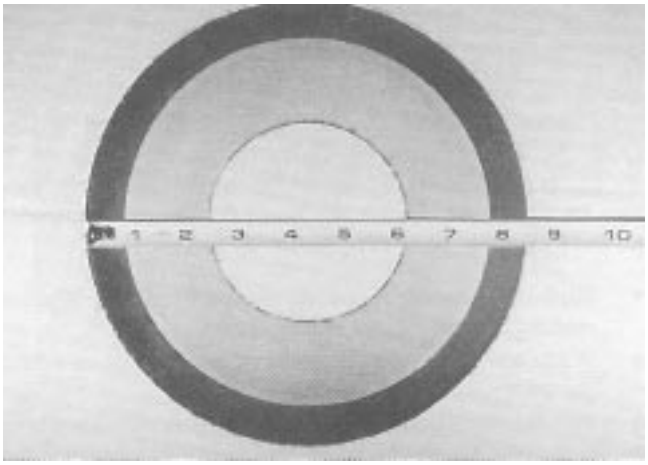

Fig. 2 Cross section of Casting 10 at mid-length, showing uniform SS310 outer layer and T-11 inner layer. The stainless layer appears darker than the T-11 layer because of dark-field photography of the macroetched ring. 0.26×

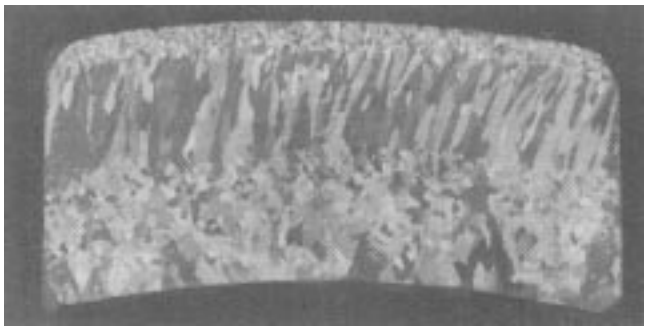

Fig. 3 Cast structure of SS310 layer in Casting 10 at mid-length. 50% HCl + H_2O_2 in H_2O. 2×

Figure 2 depicts a ring taken at mid-length from Casting 10, the casting from which most of the extruded test material described in this article originated. Measurements made on three or four rings from every casting showed that the outer layer, clearly discernible in Fig. 2, is quite uniform in thickness around the circle, and from end to end of the casting, except for three castings in which slight-to-heavy meltback of the SS310 layer occurred during pouring of the T-11 layer. Except for those castings with the undesirable meltback, the two layers are not metallurgically bonded together, owing to oxidation of the inner surface of the SS310 layer before the T-11 layer is poured. (A certain amount of beneficial mechanical interlocking develops between the layers, however, as the molten T-11 enters shrinkage pores and conforms to other minor irregularities in the SS310 surface.) The cast structure of the SS310 layer of Casting 10 at mid-length is presented in Fig. 3. In going from the pouring end to the opposite end, the columnar grains give way to equiaxed grains at the outer and especially at the inner surfaces of the stainless layer. Hardness profiles measured through the full wall of Casting 10 are presented in a later section.

3. Extrusion

The conversion of billets from bimetallic castings into clad tubes were conducted in two campaigns using six billets each. In the first campaign, billets 0.46 m (18 in.) in length were cut from the two best castings; these were turned to an outer diameter of 203 mm (8 in.). This necessitated removing more of the stainless layer than would be necessary just for cleanup, because the casting, made in an existing mold, had an OD somewhat greater than would be used in an optimized process. After machining the bore surface of the casting and machining a "nose" radius at the outer edge of one end, the boundary between the two layers was seal welded to prevent oxidation along the mating surfaces of the outer and inner layers during soaking for extrusion.

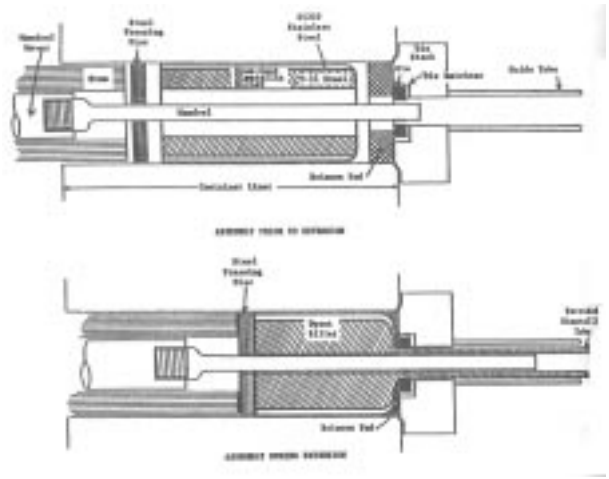

Fig. 4 Extrusion of a clad tube (schematic). Upper drawing shows annulus that existed between mandrel and billet before initial upsetting stage.

Extrusion was conducted in a 5500-ton horizontal press. The extrusion of 51-mm (2-in.) tube is illustrated schematically in Fig. 4. A billet preheated at 1175 °C (2150 °F) in a gas-fired furnace was coated with fritted glass and placed in the chamber of the press, in which an 210 mm (8.25 in.) ID container liner had been installed. Because the ID of the machined billet was about 100 mm (4 in.), a relatively large annular gap existed between the 38-mm (1.5-in.)-diameter mandrel and the billet. This large gap was atypical of good extrusion practice, but proved to cause no serious problems. The billet appeared to have been upset uniformly to fill this annulus at the start of the extrusion stroke, without developing undulations, corrugations, or laps on the inner surface, and the steel pressing disc kept the upset billet from back-extruding into the space between the mandrel and the stem. As the stem advanced toward the right in Fig. 4, a glass fiber pad helped guide the bimetallic billet into the die opening and also supplied glass lubricant to help prevent tearing of the extrusion surface. A steel guide tube helped assure straightness of the exiting tube. Because the large initial annulus between the billet and mandrel prevented use of a carbon follower block, it was not possible to exhaust the full billet from the chamber. Instead, the extrusion stroke was ended when the pressing disc neared the glass pad (or steel cone, for those extrusions made with a conical tool steel die lead-in instead of a glass pad), thus leaving a small remnant of the billet in the chamber, to be removed with the built-in cutoff wheel mounted on the press.

The first four extrusions were made with tooling that produced tubes 84 mm (3.3 in.) in OD and 64 mm (2.5 in.) in ID, the extrusion ratio being 13.4. One of these was made with a steel cone lead-in, while the remaining three were made with glass pad lead-ins to the die. This intermediate size tube was to be cold Pilgered to 51-mm (2-in.) tube in the event that direct extrusion of such tubes was unsuccessful, but this proved to be unnecessary. The last two extrusions were 51-mm (2-in.)-diameter tubes, both made with glass pad lead-ins. These had an extrusion ratio of 37.6. The 84-mm (3.3 in.) tube was about 4.6 m (15 ft) in overall length, whereas the 51-mm (2-in.) tube had

Table 1 Chemical compositions of bimetallic castings

Casting	Sample	Composition(a), %						
		C	Mn	Si	Cr	Ni	Mo	N
SS310								
3	Melt	0.02	0.54	0.31	24.89	21.89	…	0.101(b)
5	Melt	0.02	0.46	0.22	25.05	21.76	…	0.084(b)
9	Melt	0.01	0.39	0.23	25.35	21.79	0.13	0.04
	Tube	0.03	0.15	0.21	26.06	22.09	0.13	…
10	Melt	0.06	0.48	0.24	24.62	21.70	0.08	0.07
	Tube	0.06	0.23	0.25	24.47	23.39	0.12	…
T-11								
3	Melt	0.11	0.29	0.60	1.55	0.01	0.36	…
	Tube	0.11	0.27	0.57	1.61	0.15	0.38	0.067
5	Melt	0.09	0.44	0.87	1.55	0.01	0.46	…
	Tube	0.08	0.42	0.87	2.71	1.18	0.52	0.073
9	Melt	0.07	0.44	0.84	1.27	0.01	0.26	…
	Tube(c)	0.08	0.39	0.69	1.18	0.11	0.44	…
10	Melt	0.06	0.44	0.70	0.95	0.01	0.67	…
	Tube	0.08	0.51	0.67	1.02	0.08	0.69	…

Note: Samples contained 0.012 to 0.046% P and 0.004 to 0.017% S. (a) bal Fe. (b) Nitrogen sample was from tube. (c) The T-11 layer of this casting (flux addition) contained 0.0020% B at mid-thickness and 0.0004% B near ID surface.

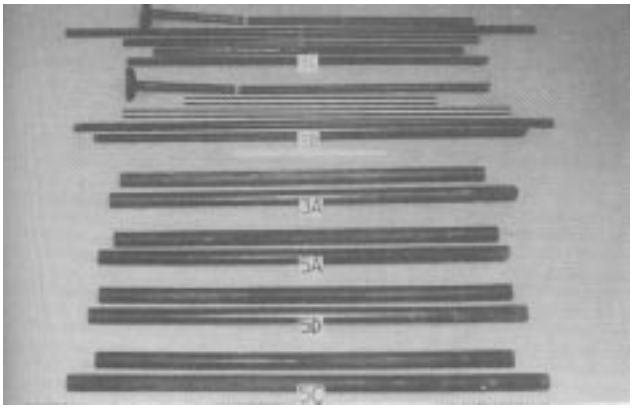

Fig. 5 The six tube produced in the first extrusion campaign. The four 84-mm (3.3-in.) tubes are in the foreground and the two 51-mm (2-in.) tubes are at the rear. Note yardstick at Tube 3B.

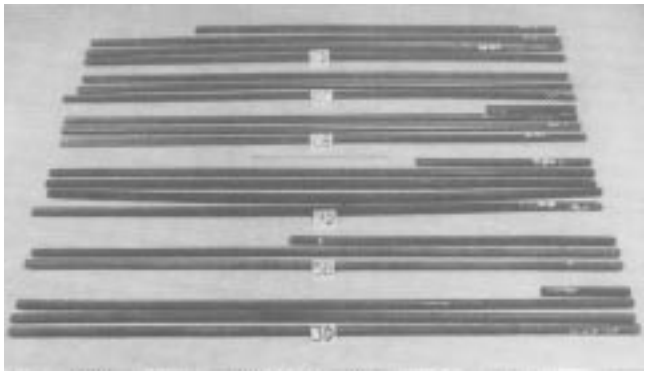

Fig. 6 Six tubes produced in the second extrusion campaign. Each of these 51-mm (2-in.) tubes had been cut into 3.7-m (12-ft) lengths. Note meter stick behind Tube 9D; this tube, made from a billet 0.66 m (26 in.) long, had an overall length of 15.8 m (52 ft), the longest of all extrusions.

an overall length of 11.9 m (39 ft). However, the clad length of each was less, because the SS310 layer of the billet, being somewhat removed from the die opening, did not exit the die at the very start of extrusion. All extrusions from the first campaign, cut mainly into 2.4-m (8-ft) lengths, are shown in Fig. 5.

In the second extrusion campaign, six billets 0.46, 0.51, and 0.66 m (18, 20, and 26 in.) in length (two each) were extruded to 51-mm (2-in.) OD × 38-mm (1.5-in.) ID tubes. Extrusion conditions were essentially the same as in the first campaign, but more of the billets (three) were extruded with steel cone die lead-ins. The six extrusions, cut into 3.7-m (12-ft) lengths, are shown in Fig. 6. Close-ups of two of these tubes, both extruded from billets taken from Casting 10 of the second campaign, are shown in Fig. 7. The upper tube was extruded with a steel cone lead-in, while a glass pad lead-in was used for the lower tube. The lower tube had a somewhat speckled appearance resulting from the glass pad. Despite the high extrusion ratio used for these tubes, both are free of surface defects, as was typical for all tubes of both campaigns extruded at 1175 °C (2150 °F). Only Tube 10D, extruded at 1090 °C (2000 °F), developed some shallow tears during extrusion, because of lower ductility at this temperature. (Tubes are identified by the casting number, followed by a letter—A, B, C, or D—denoting lengthwise position in the casting, of the billet from which the tube was extruded.)

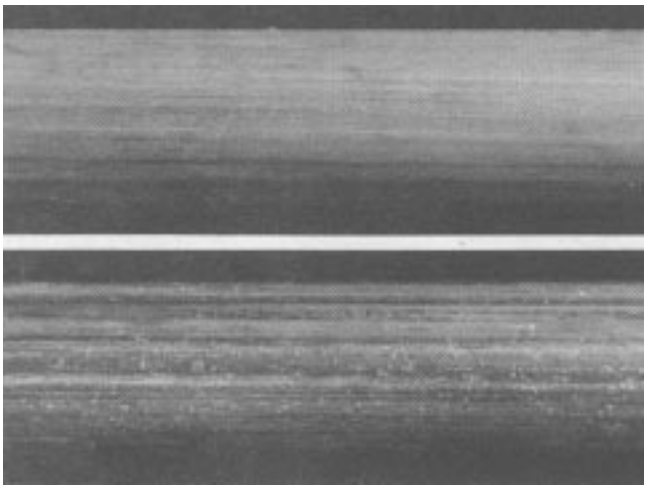

Fig. 7 Close-up views at mid-length of 51-mm (2-in.) tubes extruded with a steel cone (Tube 5B, upper) and glass pad (Tube 10C, lower). 0.43×

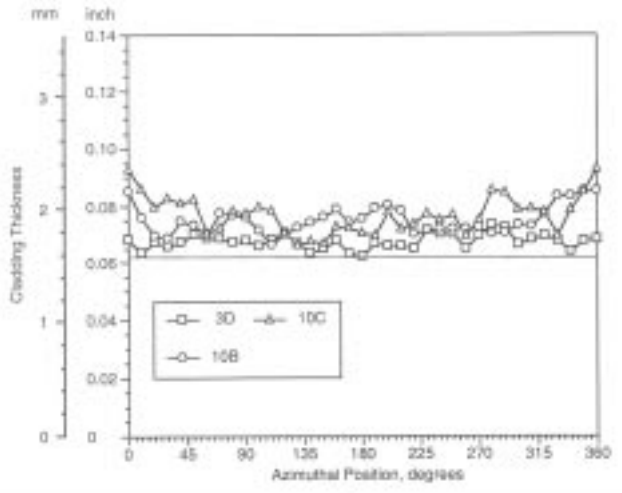

Fig. 9 Variation in cladding thickness around the circumference in rings taken at mid-length from 51-mm (2-in.) Tubes 3D, 10B, and 10C. Horizontal line denotes minimum desired cladding thickness, 1.6 mm (1/16 in.)

4. Evaluation of Clad Tubes

4.1 Uniformity of Dimensions

All tubes were subjected to precision measurements of cladding and wall thickness and of tube diameter, using a micrometer microscope fitted with a specially constructed rotating stage. In all, 43 rings from representative areas of tubes were

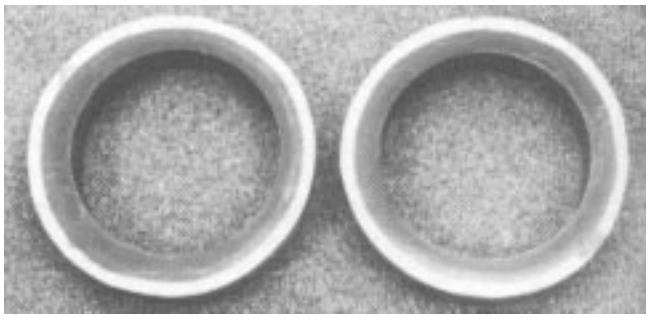

Fig. 8 Polished 51-mm (2-in.) rings from Tubes 10B (left) and 10C (right). The notch at the top is a reference mark denoting top of tube during extrusion. The T-11 layer was blued by heat tinting to facilitate measuring the uniformity of cladding thickness. Rings tilted 20° for bright-field reflection. 0.76×

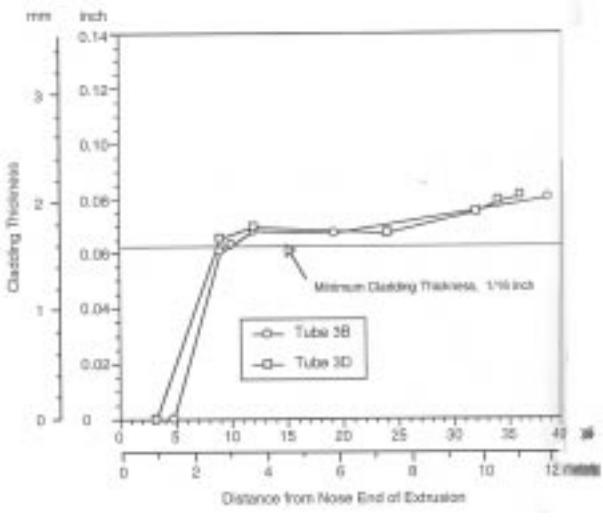

Fig. 10 Variation of mean cladding thickness along the length of 51-mm (2-in.) tubes produced from Casting 3 of the first casting campaign. Tube 3B was extruded in the first campaign with a glass-pad die lead-in and Tube 3D in the second campaign with a steel-cone lead-in.

first polished and heat-tinted (Fig. 8), to facilitate the measurement of cladding thickness. Figure 9 illustrates the variation of cladding thickness at mid-length in three 51-mm (2-in.) tubes from the second extrusion campaign. Tube 3D, made with a steel cone lead-in, has the most uniform cladding thickness; the greater variation in cladding thickness for Tubes 10B and 10C, extruded with glass pad lead-ins, may result from imperfectly sized pads, coupled with the rather large annulus between mandrel and billet. The cladding thickness of all three tubes at mid-length exceeds the desired 1.6-mm (1/16-in.) minimum thickness.

Cladding uniformity along the length of tubes may be judged from Fig. 10 and 11, in which average cladding thickness is plotted versus lengthwise position in the tube. The cladding starts approximately 1.2 m (4 ft) from the nose end, reaches the desired 1.6-mm (1/16-in.) minimum thickness about 2.4 m (8 ft) from the end, and exceeds the minimum along the remainder of each tube. The two tubes in Fig. 10, originating in Casting 3 of the first campaign, but extruded in the second campaign, show good uniformity along the length, with mild thickening of the cladding near the tail end of the tube.

Figure 11 represents tubes taken from Casting 10 of the second campaign. One of the tubes (10B) has a short initial thick zone attributed to the glass pad and shows marked thickening near the tail end of the extrusion, most likely because the SS310 layer of the billet tends to "bunch up" somewhat behind the glass pad. Nearly complete extrusion of Billet 10B thus led to the thick cladding. Lesser exhaustion of Billet 10C from the extrusion container avoided such thickening. Such marked thickening at the tail end can be avoided with steel cone lead-ins to the die. Some examples of tube yields, computed by comparing the weight of the tube having a cladding thickness of at least 1.6 mm (1/16 in.) to the billet weight, are 72% for Tube 3D [0.46-m (18-in.) billet], 74% for Tube 10B [0.51-m (20-in.) billet], and 79% for Tube 9D [not shown in Fig. 10 and 11, 0.66-m (26-in.) billet]. Because end losses are the same for all billet lengths, tube yield rises significantly as billet length increases.

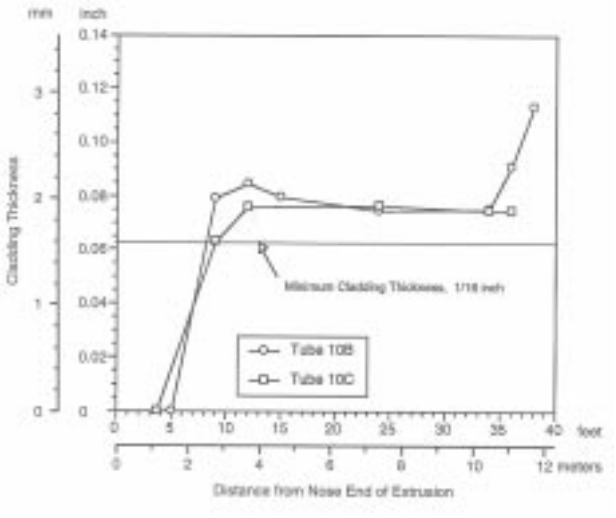

Fig. 11 Variation of mean cladding thickness along the length of 51-mm (2-in.) tubes produced from Casting 10 of the second casting campaign. Both Tubes 10B and 10C were extruded with glass-pad lead-ins.

Some variation in wall thickness around the circumference was detected, but the observed variation is not considered excessive for seamless tube. Optimization of billet shape and dimensions, and of the extrusion tooling, should reduce such variation to negligible levels. Tube diameter tends to increase slightly in about the middle half of the tube because of a mild upsetting action as this hot metal pushes the metal ahead of it along the runout table. Because all tubes of the second campaign were produced with the same extrusion die, a slight increase in tube diameter from one tube to the next was caused by die wear.

4.2 Microstructure

Close-up views of the bond line of Tube 10C are provided in the SEM micrographs of Fig. 12. Chromium oxide, which had formed a continuous film on the inner surface of the SS310 layer before the T-11 was poured, exists as isolated particles in the extruded tube, the two alloys being metallurgically bonded together between particles. This is because of the great expansion of interface area during the extrusion process that fragments the oxide film, permitting the SS310 and T-11 to be

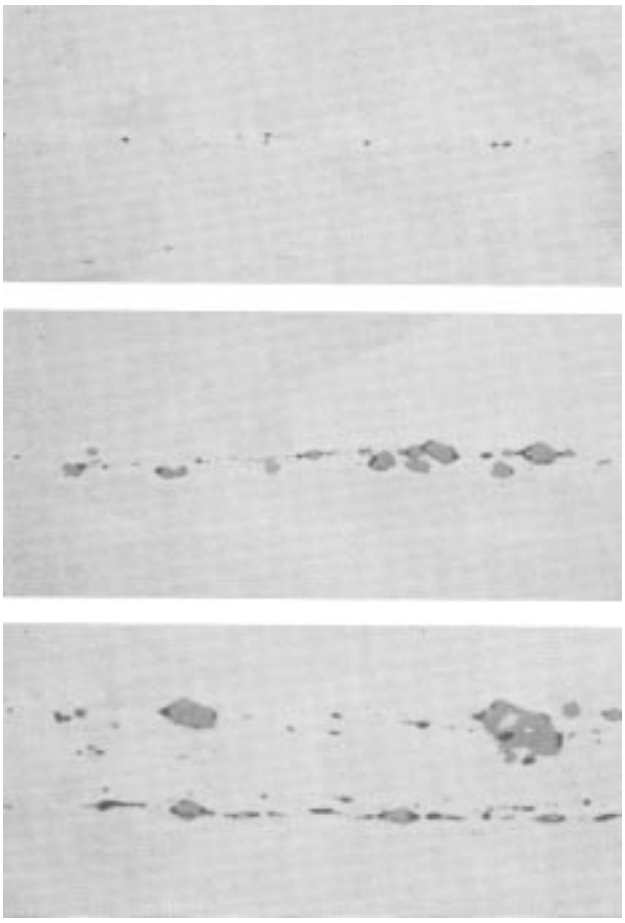

Fig. 12 Scanning electron micrographs of bond-line inclusions in as-extruded Tube 10C. These photographs illustrate the range of oxide inclusion density in a longitudinal section taken at mid-length of the tube. The two metallic layers were welded together between the particles during extrusion. Unetched, back-scattered-electron (BSE) images. 1000×

welded together between particles as the billet passes through the extrusion die. Such bonding occurs even in heavy oxide zones, as seen in the middle and lower photographs in Fig. 12. The disposition of the numerous shrinkage pores that exist on the inner surface of the SS310 layer at the end of solidification is illustrated in Fig. 13. The T-11 that fills the pore is flattened into a low mound during extrusion. Oxide that forms in the many microshrinkage pores around the main pore may be seen as a thin cloud of particles near the mound. Such porosity zones have been well amalgamated into the bond-line structure and are considered harmless.

The microstructures of the two layers of as-extruded Tube 10C adjacent to the bond line are shown in Fig. 14. The SS310 layer consists of uniform equiaxed grains throughout the thickness, of ASTM 7 size. A cluster of oxide particles from a pore zone exists adjacent to the bond line. The T-11 layer is observed to have been slightly decarburized during the extrusion process, the carbon having diffused into the SS310 layer. Below this layer, the main structure of the T-11 base metal consists of proeutectoid ferrite and bainite, as is typical for air-cooled tubes of Cr-Mo low-alloy steels.

Tube samples were full-annealed [930 °C (1700 °F), 1 h, furnace cool] to place them in conformance with the ASME Boiler Code. The microstructures of the tube alloys are depicted in a through-thickness series of each layer of Tube 10C shown in Fig. 15. The SS310 layer is essentially the same as in the extruded condition; grain size again is ASTM 7, showing that the recrystallization that occurred after extrusion had developed a fine, stable grain structure that was not affected by annealing. Adjacent to the bond line a dark band approximately 0.025 mm (0.001 in.) thick may be seen, representing fine carbides that formed as a result of carbon diffusion from the T-11 layer into the SS310 layer during annealing. These carbides promote fine cracking in this zone during heavy deformation (i.e., in the necked zone of a bimetallic tensile specimen), but should not cause cracking during normal fabrication of tubes. If necessary, the extent of the carburized zone could be minimized by annealing at lower temperatures or for shorter times, or by use of subcritical annealing.

Decarburization occurring in the T-11 base metal, resulting from this outward carbon diffusion into the SS310, is shown in the lower half of Fig. 15. This zone is approximately 0.6 mm (0.025 in.) thick, or 13% of the T-11 thickness. Below this layer, the T-11 base metal consists of ferrite and pearlite. The amount of pearlite increases significantly near the inner surface of the tube. This results from two factors: (1) an 0.03% C through-thickness increase in the carbon content of the cast T-11 layer (possibly caused by segregation induced by the high centrifugal force) and (2) carbon pickup at the bore surface of the T-11 billet during soaking for extrusion, emanating from carbon plugs in the billet. Although the decarburized band of ferrite would exhibit somewhat lower stress-rupture properties than T-11 of normal carbon content, as shown by Sponseller et al. for the similar T-22 steel (Ref 3), this effect would tend to be offset by the benefits of the higher carbon zone near the inner surface.

For as-extruded as well as annealed tubes, there is little difference in microstructure of the SS310 and T-11 layers (1) from end to end of a tube, (2) between different tubes (A, B, C, or D) from the same casting, or (3) between tubes from different castings.

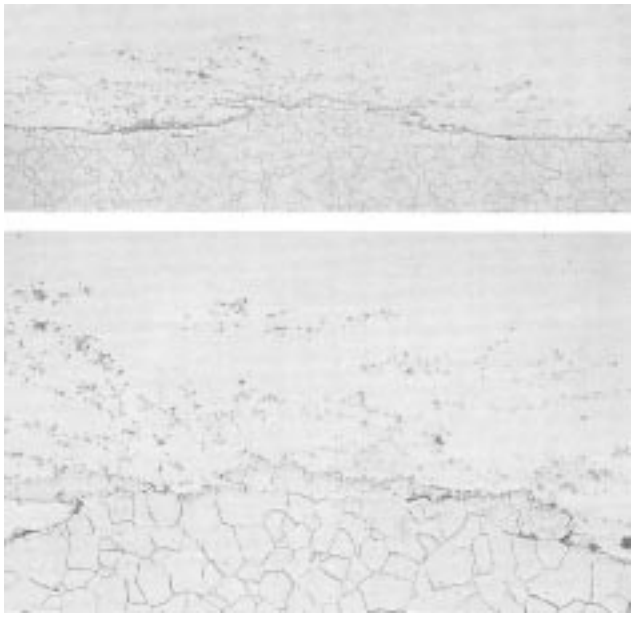

Fig. 13 Transverse section through extruded Tube 10C at site of shrinkage pore in the ID surface of as-cast SS310. Pore was filled in by the molten T-11 and flattened into a low mound during extrusion. Cluster of oxide particles originated in microshrinkage pores surrounding the main pore. Nital etch, 50× (upper), 150× (lower)

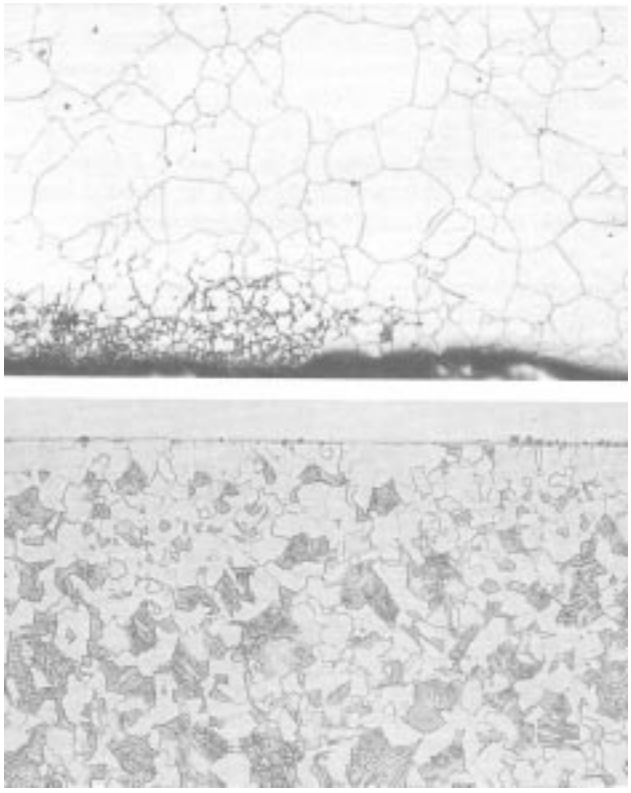

Fig. 14 Microstructure of as-extruded Tube 10C, showing SS310 layer (upper) and T-11 layer (lower), both adjacent to the bond line. Upper: transverse, 50% HNO_3 (electrolytic), 200×; lower, longitudinal, Nital, 100×

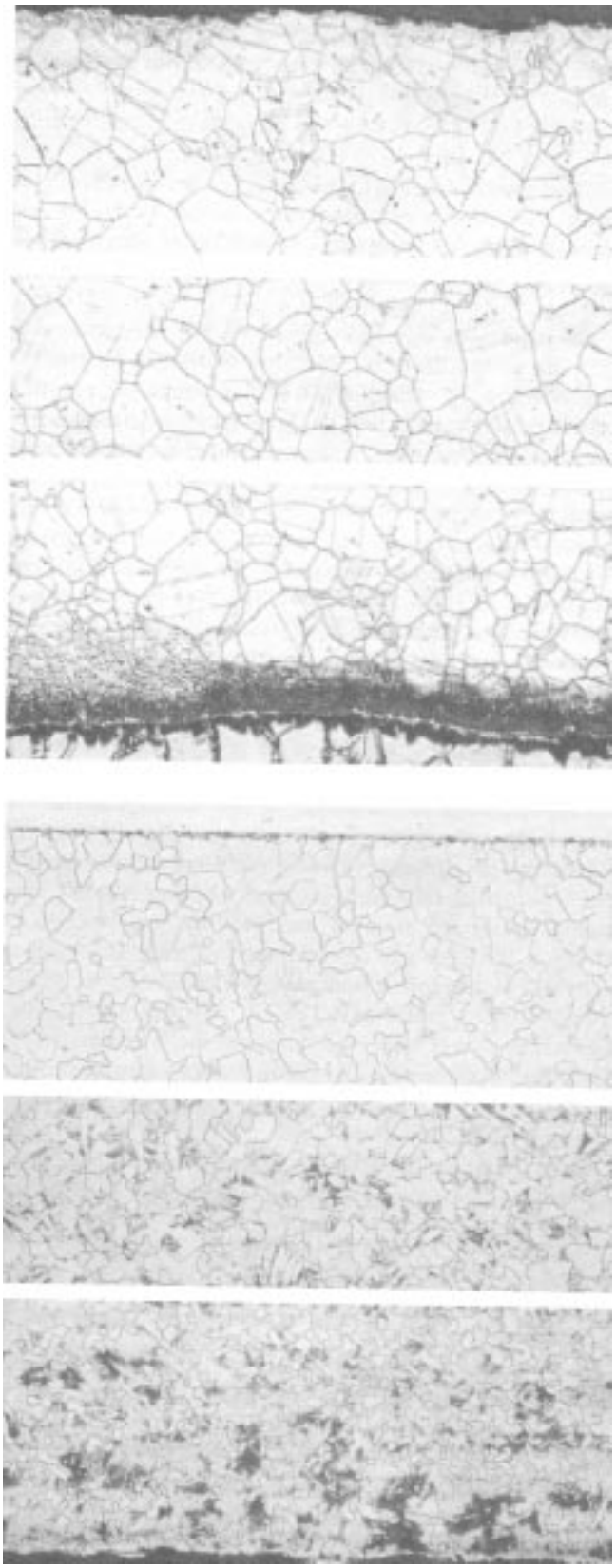

Fig. 15 Microstructure of annealed Tube 10C, as shown in through-thickness series of the SS310 (upper) and T-11 (lower). For each layer, the outer, mid-thickness and inner regions are depicted. Upper: transverse, 50% HNO_3 (electrolytic), 200×. Lower: longitudinal, Nital, 100×

Negligible diffusion of substitutional alloying elements occurs between layers, as seen in a cross section of annealed Tube 10C (Fig. 16). The nickel distribution in the two layers shown on either side of the bond line in the SEM photograph at the left is illustrated in the nickel x-ray dot map at the right; a sharp demarcation is evident.

4.3 Mechanical Behavior

Radial hardness profiles in the bimetallic tubes, measured at the various stages of production, are compared in Fig. 17 to 19. Profiles at four locations along the length of Casting 10 are quite similar. The SS310 has a hardness of about 120 HV, increasing slightly near the T-11 layer. At three of the lengthwise locations, the hardness profiles in the T-11 are essentially identical, increasing moderately (from 140 to 185 HV) proceeding inward. This radial hardness variation in the T-11 is attributed primarily to the 0.03% C increase noted earlier. The hardness profile of the section near the T-11 pouring end lies slightly above the others.

Figure 18 presents hardness profiles of as-extruded tubes, at three locations in Tube 10C and at mid-length of Tubes 9D and 10B. Grain refinement during extrusion raises SS310 hardness by 20 HV points to 140 HV; there is little difference between the five sections. Because carbon is present in the form of bainite, not coarse pearlite, the T-11 base metal of as-extruded tubes is appreciably harder than the SS310 cladding, most readings lying between 180 and 210 Hv. Hardness at each location is nearly constant throughout most of the thickness, but increases appreciably near the inner surface, reflecting the effect of the increased carbon content on bainitic hardenability. The relatively high hardness in most of the T-11 layer of Tube 9D results from a fully bainitic structure caused by boron pickup from the flux used for Casting 9.

Figure 19 shows that annealing has no effect on the SS310 hardness, but markedly lowers that of the T-11, to a level somewhat below its as-cast hardness (especially near the inner surface), because of coarse pearlite developed during furnace cooling. The decarburized band of T-11 next to the bond line is indicated by slightly lower hardness. The peak hardness values shown in Fig. 19 represent the average of six microhardness readings made with the Knoop indentor aligned directly on the bond line. (No such readings were made on as-extruded tube sections.) Though oxide particles on the bond line probably contribute a small amount to these hardness values, the peak in

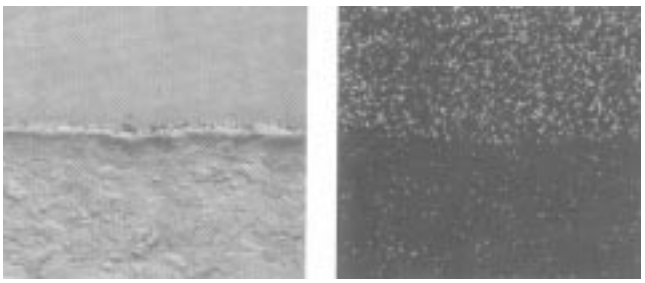

Fig. 16 Bond-line region of annealed Tube 10C at mid-length, showing a SEM photograph (BSE image), left, and Ni x-ray dot map taken at the same location, right. Transverse section, 50% HNO_3, 100×

hardness—about 45 HV above the cladding hardness—is attributed mainly to the 0.025-mm (0.001-in.)-thick band of fine carbides, shown in Fig. 15, that developed in the cladding during annealing. In summary, the hardness profiles reveal (1) soft as-cast austenite, hardened somewhat by extrusion but unaffected by annealing, except for a very thin band at the bond line hardened by carbide precipitation during annealing, (2) relatively soft T-11 in the casting that becomes moderately harder during air cooling following extrusion, and then becomes quite soft during annealing, and (3) hardness that is uniform: over the length of a casting or extrusion, from one tube to another, and generally through the thickness of each layer, with a moderately higher hardness near the inner surface of the T-11 in the as-cast and the as-extruded states.

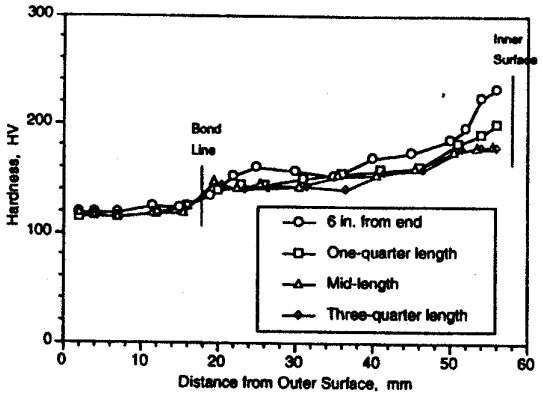

Fig. 17 Hardness variation of Casting 10 measured through the wall along a radial line, at the four indicated sections with respect to the T-11 pouring end. Converted from HRA

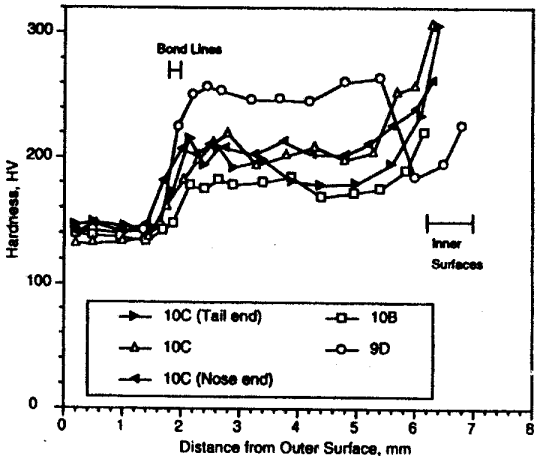

Fig. 18 Hardness variation at mid-length of three as-extruded 51-mm (2-in.) clad tubes measured through the wall along a radial line. Tube 10C was also tested at the nose and tail ends. The ranges of bond-line and inner surface positions are indicated by horizontal lines. Converted from Knoop (2000 g)

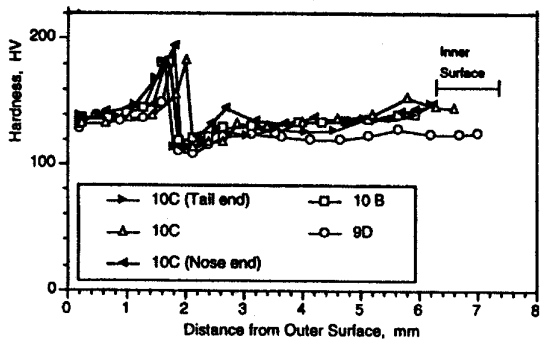

Fig. 19 Hardness variation of annealed tubes, measured through the wall, at the same locations as in Fig. 18. Converted from Knoop (2000 g)

Annealed tubes were subjected also to bulk hardness measurements, using HRB tests. Specimens representing a wide variety of processing variables (two casting campaigns, non-flux and flux casting practice, various billet locations in the casting, two extrusion campaigns, steel-cone and glass-pad extrusion die lead-ins, and various locations of hardness specimens in extruded tube) were tested, producing results listed in Table 2. Hardness values of the SS310 layer are quite uniform, and the 75.6 HRB average lies well below the 90 HRB maximum specified in ASTM A 213 (Ref 4). The T-11 hardness values show somewhat greater variation, which is probably due to low manganese and molybdenum concentrations in the softer specimens. The average T-11 hardness, 72.8 HRB, lies well below the 85 HRB upper limit given in ASTM A 213. Tensile specimens of annealed T-11 were prepared from companion material to all the above specimens, except for Tube 9D; blanks had been flattened before annealing. The results, presented in Table 3, are quite uniform, with average values of 289 MPa (41.9 ksi) yield strength, 489 MPa (70.9 ksi) tensile strength, 29.5% elongation, and 68.5% reduction of area. These values readily satisfy the strength and ductility requirements of ASTM A 213. Full-wall (composite) bimetallic tensile specimens also were prepared from annealed stock of Tubes 3B and 10C. The results, presented in Table 4, show that all properties, except reduction of area, exceed those of the T-11 given in Table 3. This helps build a case for including the strengthening contribution of the cladding when computing tube wall thickness under the ASME Boiler Code.

Bond shear strength was measured on four specimens of the lap-shear type. One such specimen, photographed just before

Table 2 Bulk hardness of SS310 and T-11 layers of annealed 51-mm (2-in.) tubes

Tube No.	Location in extruded tube	Hardness, HRB(a)	
		SS310	T-11
3B	Mid-length	74.2	71.3
3D	Mid-length	74.5	69.6
9D	Mid-length	75.1	69.8
10B	Mid-length	75.3	74.2
10C	Nose end	76.4	74.8
	Mid-length	77.3	75.5
	Tail end	76.5	74.3
Average		75.6	72.8
ASTM A 213 specification		90 max	85 max

(a) Average of five tests

failure while withstanding a shear stress of 168 MPa (24.3 ksi), is shown in Fig. 20. The spreading, and deformation at the root, of the thin slots provides some indication of the heavy stress state in the specimen. Shear strengths range from 127 to 230 MPa (18.4 to 33.3 ksi). Such tests are quite sensitive to test conditions because the very short plastic zone provides little accommodation of any misalignment; thus, even higher values would be expected under ideal test conditions. The fracture surface of the T-11 side of such a specimen is shown in the lower photograph of Fig. 20. Most of the fracture surface follows the bond line, but the lighter areas represent fracture through the softer T-11 layer. The ridged nature of the bond line interface between the two alloys should provide better mechanical strength to resist thermal and applied stresses than would a smooth interface.

Table 3 Tensile properties of annealed T-11 base-metal specimens from 51-mm (2-in.) tubes

Tube No.	Location in extruded tube	0.2% Offset yield strength, MPa	0.2% Offset yield strength, ksi	Tensile strength, MPa	Tensile strength, ksi	Elongation, %	Reduction of area, %
3B	Mid-length	289	41.9	472	68.4	30.2	66.7
		285	41.3	463	67.2	28.1	66.4
	Average	287	41.6	467	67.8	29.0	66.5
3D	Mid-length	295	42.8	471	68.3	29.5	67.5
		291	42.2	462	67.0	30.4	63.6
	Average	293	42.5	467	67.7	30.0	65.5
10B	Mid-length	244	35.4	479	69.5	32.5	69.7
		296	42.9	507	73.5	29.2	67.8
	Average	270	39.2	493	71.5	31.0	69.0
10C	Nose end	293	42.6	502	72.8	27.1	67.7
		293	42.5	508	73.7	27.4	70.8
	Average	293	42.6	505	73.3	27.5	69.5
10C	Mid-length	281	40.8	505	73.2	29.2	70.2
		294	42.7	503	73.0	30.4	69.2
	Average	288	41.8	504	73.1	30.0	69.5
10C	Tail end	301	43.6	496	71.9	29.7	68.6
		301	43.6	499	72.4	29.4	70.6
	Average	301	43.6	498	72.2	29.5	69.5
Average for all tests		**289**	**41.9**	**489**	**70.9**	**29.5**	**68.5**
ASTM A 213, grade T-11 specification		207 min	30 min	414 min	60 min	22.5 min(b)	…

Note: Blanks were flattened at 700 °C (1300 °F), machined to remove SS310, held in a protective atmosphere at 925 °C (1700 °F) for 1 h, furnace cooled, and machined to tensile specimens. (a) For 3.8-mm (0.150-in.) thick test specimen

Table 4 Tensile properties of annealed full-wall bimetallic specimens from 51-mm (2-in.) tubes

Extruded tube	Location in tube lengthwise	T-11 % of wall thickness	0.2% Offset yield strength, MPa	0.2% Offset yield strength, ksi	Tensile strength, MPa	Tensile strength, ksi	Elongation, %	Reduction of area, %
3B	Middle	72	296	43.0	515	74.7	33.3	54.1(a)
			297	43.1	514	74.5	34.5	55.1(a)
	Average		297	43.1	514	74.6	34.0	54.5
10C	Middle	68	317	46.0	545	79.1	32.7	56.7(a)
			317	46.0	560	81.2	31.4	52.7(a)
	Average		317	46.0	553	80.2	32.0	54.5
Average for all tests			307	**44.6**	**534**	**77.4**	**33.0**	**54.5**
ASTM A 213, grade T-11 specification			207 min	30.0 min	414 min	60.0 min	29.5 min	…

Note: Blanks were flattened at 700 °C (1300°F), held in a protective atmosphere at 925 °C (1700 °F) for 1 h, furnace cooled, and machined to full-thickness tensile specimens. (a) Based on overall final dimensions of fracture. A higher value would be obtained if cross-sectioned area of small gap that developed between layers at the fracture were subtracted from final area.

Another means of assessing bond shear strength, developed during this study, is the twist test. This involves preparing Blanchard-ground and heat-tinted rings 3.1 mm (0.125 in.) in thickness, with a radial slot, as shown at the left in Fig. 21, upper. One end by the slot is placed in a vise and twisted 90° with a special tool. The process is then repeated at 12.7-mm (1/2-in.) intervals around the full circumference (11 twists in all), producing spiral bimetallic rods such as those shown in Fig. 21, upper. The force-couple imposed by the twisting tool and the vise jaws develops a high shear stress along the bond line, especially near the pressure points denoted by the dimples at the OD surface (Fig. 21, lower). The lengths of any small fissures and cracks are measured under a binocular microscope. Alternatively, twists of increasing severity, up to 160°, are made to determine the critical twist angle necessary to cause fissures or cracks of any given size. In all, 24 twist tests of the two types were performed. Except for rings of Tube 9D produced from flux-treated Casting 9 and weakened by residual flux at the bond line, cracking at the bond line was quite minor. In rings uniformly twisted 90°, small fissures occupied only 3%, on average, of the twist-tested length of the bond line of tubes produced from non-flux-treated castings. All of these fissures were at the pressure points. The fact that the bond line between the pressure points withstood the severe twisting stresses without cracking attests to the good metallurgical bond between the cladding and base metal. In rings from flux-treated casting , the 90° twist tests caused cracks along 14% of the bond line in specimens from the nose end of the extrusion, and 74% at the tail end, indicating that some residual flux between the two layers was squeezed rearward during the extrusion. Clearly, flux treatments are not needed for, and can be detrimental to the attainment of, good bonding between the layers.

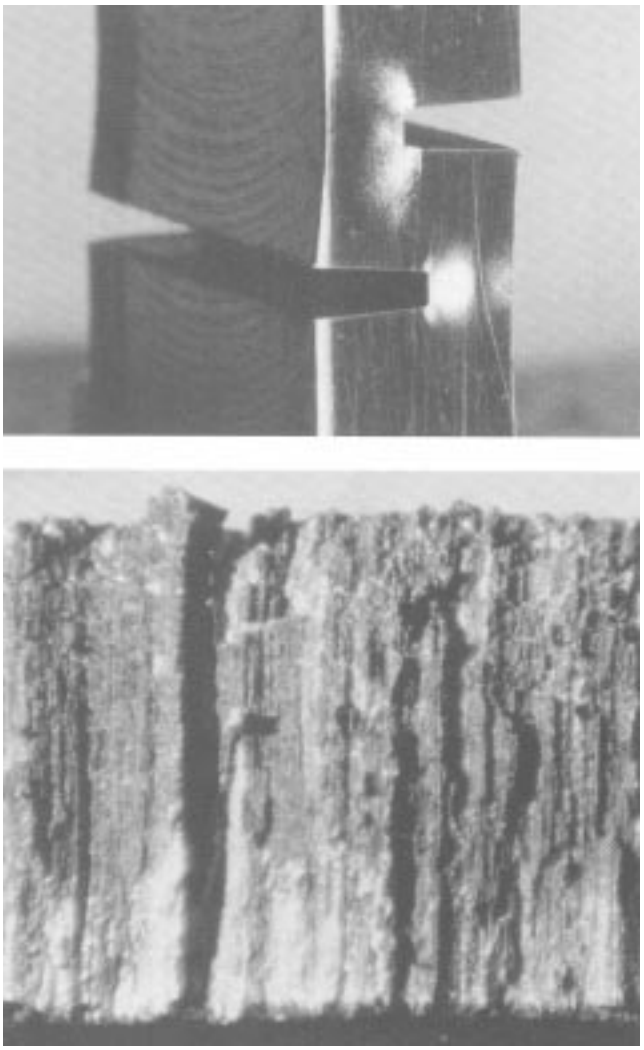

Fig. 20 Bond-shear strength test specimen from annealed Tube 10B, slotted to induce failure at the bond line. Upper: pictured at a shear stress of 168 MPa (24.3 ksi) just before failure, 4.5×. Lower: T-11 side of fracture surface, shadowed to highlight ridges. 15×

Annealed tube specimens from the nose and tail ends of Tubes 10B and 10C passed both stages of the ASTM A 450 flattening test (Ref 5). The 64-mm (2.5-in.)-long tube from the nose end of Tube 10B, flattened under a maximum load of 39 tons, is shown in Fig. 22. It experienced only small fissures at the bond line in several, but not all, severely deformed "corners" of the specimen. Other annealed tube specimens from the same locations (not shown here) passed the ASTM A 450 flaring test.

The results presented in this section suggest that tubes produced from centrifugally cast bimetallic billets has ample ductility and bond-line adhesion between layers to withstand fabrication operations and the thermal stresses encountered in service, while meeting the hardness and tensile requirements for the two alloys.

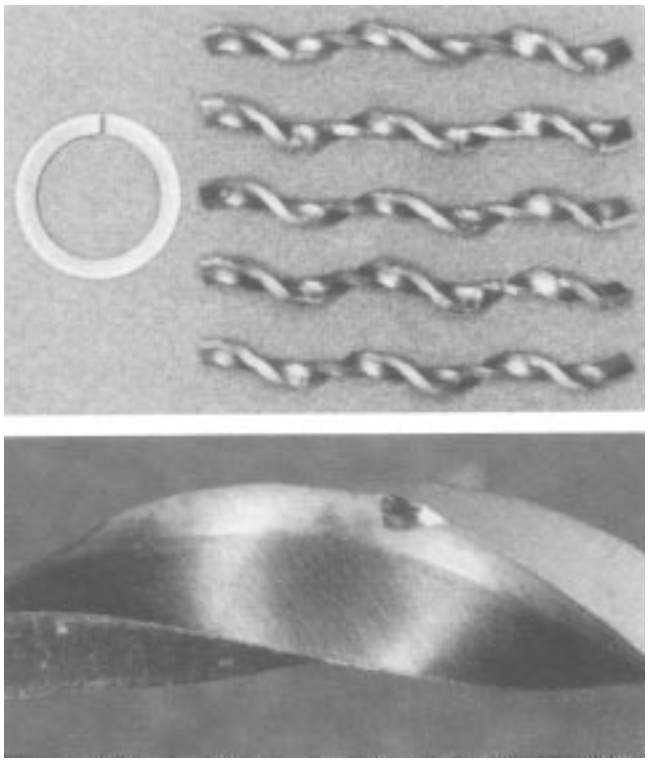

Fig. 21 Before and after views of twist test rings. Upper: a slotted, but untested, ring and five tested rings, taken from three annealed 51-mm (2-in.) tubes, 0.43×. Lower: close-up of ring 3B; dimples represent pressure points for the 9th and 10th 90° twists. 3.3×

5. Cost Analysis for Commercial-Scale Production of Clad Tubes

Cost estimates are presented here for the commercial-scale production in the U.S. of 51-mm (2-in.) OD × 38-mm (1.5-in.) ID tubes of the present type, i.e., T-11 steel clad with a 1.6-mm (1/16-in.) layer of SS310. Pricing is based on actual quotations for processing in the same full-scale commercial centrifugal casting and extrusion facilities used in this investigation, and for two operations—(1) commercial heat treating, straightening, inspection, and (2) possible cold Pilgering, both with deglassing as necessary—not used in this developmental study. It was assumed that basically crack-free tubes could be extruded from billets 229-mm (9-in.) OD × 1.02-m (40-in.) long, somewhat larger than the largest of this study (203-mm (8-in.) OD × 0.66-m (26-in.) long). If some cracks should develop, several measures are available to help eliminate such defects. Allowance was made for a 20% loss of extruded tube for scrap and trimming to length. The quotations obtained were for conducting the various operations on commercial quantities (100 castings and the resulting 300 billets) of product on a toll basis. Allowance was also made for the cost of shipping billets or tubes between production facilities and for price inflation between the dates of the quotations and at the time of this publication.

Because of severe heating of the 38-mm (1.5-in.) diameter mandrel, the extrusion quotation for 51-mm (2-in.) tube was based on the use of a new H-13 mandrel for each tube. The cold-Pilgering option involves extrusion to an intermediate size, 89-mm (3.5-in.) OD × 71-mm (2.8-in.) ID, followed by cold Pilgering to 51-mm (2-in.) OD × 38-mm (1.5-in.) ID. Although cold Pilgering was not used in this study, it is believed that slowly cooled extruded tubes would have sufficient ductility to withstand cold Pilgering to the final size. This option is presented because it offers an overall cost saving, resulting from much lower mandrel costs for extrusion (because the heavy mandrel is not overheated), while achieving certain expected advantages in product quality, such as better surface smoothness and more uniform diameter and wall thickness in the 51-mm (2-in.) tube. Besides estimating the cost using the same billet preparation as in this study (conventional billet preparation), simpler billet preparation (as-cast surface, no nose radius, no seal welding)—the viability of which needs to be established—was considered as a cost-saving option, as was the further use of a superalloy mandrel that could be used for multiple extrusions. Cost estimates are as follows:

	Price, $/m ($/ft)	
Processing conditions	Direct extrusion	Extrusion + cold Pilgering
Conventional billet preparation	140 (42.75)	120 (36.60)
Simpler billet preparation	126 (38.35)	106 (32.20)
Superalloy mandrel (8 extrusions per mandrel)	106 (32.20)	… (…)

Tube prices for conventional billet preparation, especially with the cold Pilgering option, are well below those for conventionally produced clad tubes (>$165/m, >$50/ft). Assuming that simpler billet preparation proves successful, an even greater price advantage would be realized. Still greater cost saving attends the use of a superalloy mandrel. If demand for clad tube develops to a sufficient level, all of the processing steps could be performed in one integrated plant, thereby promoting coordination of activities, eliminating shipping costs, and facilitating recycling of croppings and other scrap. Assuming that costs would be 25% lower in an integrated plant, tube costs for the processing schemes listed in this table would range from $79/m to $105/m ($24 to $32/ft).

For achieving greater hot corrosion resistance, such as for waste-incineration boilers, it may be desirable to use nickel-base cladding in place of the SS310. Although it would be necessary to first prove out the hot workability of bimetallic billets having such an outer layer (or inner layer, for the tubing of sour-gas wells), the difference in alloy cost would add less than $33/m ($10/ft) to the prices given in this table, suggesting that clad 51-mm (2-in.) tubes possessing the high surface degradation resistance of nickel-base alloys might be obtained for about $165/m ($50/ft) or less.

6. Summary

This study shows that centrifugal casting is an efficient way to unite stainless steel and base metal in the preparation of billets for the hot extrusion of clad boiler tubes. By this method, 203-mm (8-in.)-diameter billets prepared from bimetallic centrifugal castings weighing approximately 625 kg (1375 lb) were successfully hot extruded in a 5500-ton press, at a ratio of 37.6. Tubes so-produced, 51 mm (2 in.) in OD × 38 mm (1.5 in.) in ID, with a 1.6-mm (1/16-in.)-thick layer of SS310 on a T-11 steel base, are rather uniform in cladding thickness and wall thickness, and possess uniform microstructures from end to end of tubes and from tube to tube. Diffusion of carbon across the bond line during full annealing causes a decarburized band in the T-11 and a 0.025-mm (0.001-in.)-thick band of fine carbide precipitation in the SS310, that are not likely to interfere with fabrication or service performance. The SS310 becomes metallurgically bonded to the T-11 during the extrusion process. As a result, the shear strength at the bond line is rather high, and transverse rings from annealed tubes withstand severe deformation without separation of the layers during a twist test developed in this study; minute fissures occupy, on average, just 3% of bond-line length in rings from tubes made by the optimum process. The full-annealed tubes meet the hardness and tensile requirements of ASTM A 213 and the flattening and flaring requirements of ASTM A 450.

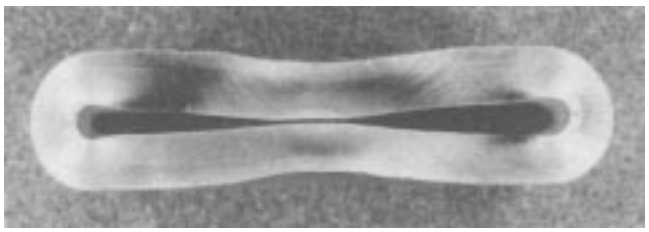

Fig. 22 Annealed flattening-test ring from nose end of Tube 10B, tested per ASTM A 450. 0.9×

Cost analysis indicates that 51-mm (2-in.) clad tubes could be produced by this process at about $106-140/m ($32 to $42/ft) and probably less in an integrated plant. This is markedly lower than the >$165/m (>$50/ft) cost for tube produced by the conventional process (i.e., extrusion of composite billets assembled from heavy-walled wrought tubes). This cost advantage could extend the use of clad tubes to applications in boilers for which the cost of such tubes has been considered prohibitive.

Acknowledgments

The principal author is deeply indebted to R.T. Delaney and R.C. Westgren for centrifugal casting expertise, V.A. Biss for exhaustive metallography, J.C. Sponseller and T.E. Sponseller for measurement and mapping of cladding thickness, hardness, and microhardness, and for performance of twist tests, R.W. McConnell for preparation of test specimens, R.M. Monroe and M.A. Zeoli for mechanical testing, K.S. Smalinskas for macrophotography, D.J. Kruzich for preparation of the manuscript, and especially to the Electric Power Research Institute, Palo Alto, CA, for sponsorship of this project (RP2742-2).

References

1. T. Flatley, E.P. Latham, and C.W. Morris, Co-Extruded Tubes Improve Resistance to Fuel Ash Corrosion in U.K. Utility Boilers, *Materials Performance,* (NACE), May 1981, p 12
2. T. Flatley, E.P. Latham, and C.W. Morris, CEGB Experience with Co-Extruded Tubes for Superheated and Evaporative Sections of PF Fired Boilers, *Proc. Conf. on Advances in Material Technology for Fossil Power Plants,* Sept 1-3, 1987, Chicago, ASM International, p 219
3. D.L. Sponseller, M. Semchyshen, and P.J. Grobner, Effects of Low-Carbon Contents and Exposures to Liquid Sodium on Elevated-Temperature Behavior of 2-1/4%Cr-1%Mo Steel, *Low-Carbon and Stabilized 2-1/4% Chromium-1% Molybdenum Steels,* 1973, American Society for Metals, p 73
4. *Standard Specification for Seamless Ferritic and Austenitic Alloy-Steel Boiler, Superheater, and Heat-Exchanger Tubes,* A 213, ASTM, Philadelphia, PA, 1992
5. *Standard Specification for General Requirements for Carbon, Ferritic Alloy, and Austenitic Alloy Steel Tubes,* A 450-94, ASTM, Philadelphia, PA, 1995